

Chemical composition and size distribution of wintertime aerosols in the atmosphere of Mt. Hua in central China

Jianjun Li^{a,b}, Gehui Wang^{b,a,*}, Bianhong Zhou^{b,c}, Chunlei Cheng^b, Junji Cao^{b,a}, Zhenxing Shen^a, Zhisheng An^{a,b}

^a Department of Environmental Science and Engineering, Xi'an Jiaotong University, Xi'an 710049, China

^b State Key Laboratory of Loess and Quaternary Geology, Institute of Earth Environment, Chinese Academy of Sciences, Xi'an 710075, China

^c Department of Geographical Science and Environment Engineering, Baoji University of Art and Science, Baoji 721013, China

ARTICLE INFO

Article history:

Received 16 September 2010

Received in revised form

16 November 2010

Accepted 1 December 2010

Keywords:

Mountain aerosols

Organic and elemental carbon

Inorganic ions

Size distribution

Sources

ABSTRACT

TSP, PM₁₀ and size-segregated aerosols were collected at the summit (2060 m, a.s.l.) of Mt. Hua in central China during the winter of 2009, and determined for organic (OC) and elemental carbon (EC), pH of water-extracts and inorganic ions. OC in TSP and PM₁₀ are 6.9 ± 2.9 and $5.9 \pm 2.5 \mu\text{g m}^{-3}$, while EC in TSP and PM₁₀ are 0.9 ± 0.6 and $0.9 \pm 0.5 \mu\text{g m}^{-3}$, respectively. SO_4^{2-} , NO_3^- , NH_4^+ and Ca^{2+} are major ions in PM₁₀ with concentrations of 5.8 ± 3.7 , 2.7 ± 1.6 , 1.6 ± 0.9 and $1.5 \pm 0.7 \mu\text{g m}^{-3}$, respectively. OC/EC ratios (8.2 ± 3.1 in TSP and 6.6 ± 1.8 in PM₁₀) at the mountaintop are 2–4 times higher than those in lowland surface, suggesting an enhanced transformation of organics from gas- to solid- phase because of an increased photochemical oxidation and/or an increased condensation due to lower temperature, as well as an increased organic input from mountain plant emission. Air mass backward trajectories showed that compared with those derived from north/northwest China aerosols transported from the south contained higher concentrations of SO_4^{2-} and NH_4^+ and lower concentrations of Ca^{2+} . Size distributions of NH_4^+ and K^+ presented as an accumulation mode with a peak at 0.7–1.1 μm , in contrast to Ca^{2+} and Mg^{2+} , which maximized at the size 4.7–5.8 μm as a coarse mode. SO_4^{2-} and NO_3^- showed a bimodal pattern with a large peak at the range 0.7–1.1 μm and a small peak at the size of 4.7–5.8 μm , whereas Na^+ and Cl^- displayed a bimodal pattern with two equivalent peaks in the fine (<2.1 μm) and coarse ($\geq 2.1 \mu\text{m}$) ranges. pH values of the water-extracts demonstrate that aerosols originate from southern China are more acidic than those from the north/northwest, and the particles with a diameter of 0.7–1.1 μm are most acidic.

© 2010 Elsevier Ltd. All rights reserved.

1. Introduction

Tropospheric aerosols are of significant impact on climate change and human health. Such effects are dependent on their chemical composition and size distribution. Atmospheric environment over mountain area is unique because of lower temperature, higher humidity and stronger solar radiation, and thus chemical and physical properties of mountain aerosols differ from those on lowlands (e.g., urban area). Furthermore, mountain aerosols are more affected by long-range transport than by local sources, and are therefore indicative of regional-scale characters of the atmosphere. Many studies on Chinese aerosols have performed at urban

sites (Yao et al., 2002; Duan et al., 2005; Sun et al., 2005; Wang et al., 2006a, b). In contrast, only a few observations were conducted at mountain sites in the country (Wang et al., 2009a, b; Xu et al., 2009), limiting our ability to obtain a panorama of air pollution in China.

Compared with that in other seasons wintertime atmospheric environment in the country is more significantly affected by coal emissions, because much more coal are burned in the cold season for house heating, adding more adsorbing soot, sulfate and organic aerosol to the Asian and Pacific atmosphere (Aldhous, 2005; Arimoto et al., 2006). Menon et al. (2002) have reported that high loadings of anthropogenic aerosols (e.g., black carbon) in central China may be responsible for the increases in the drought in the north and the flood in the south. Rosenfeld et al. (2007) further found that anthropogenic aerosols have deeply linked with the changes in the precipitation pattern in central China, specifically in Mt. Hua area. For better understanding the relationships of East Asian aerosols especially those derived from coal-burning

* Corresponding author. State Key Laboratory of Loess and Quaternary Geology, Institute of Earth Environment, Chinese Academy of Sciences, Xi'an 710075, China. Tel.: +86 29 8832 9320; fax: +86 29 8832 0456.

E-mail addresses: gehuiwang@yahoo.com.cn, wanggh@ieecas.cn (G. Wang).

emissions and their climate impacts, we characterized three types of airborne particles at the summit of Mt. Hua in central China during the winter of 2009, which are total suspended particles (TSP), PM₁₀ and size-segregated particles, respectively. In the current study we report chemical compositions and size distributions of those particles, and discuss their sources.

2. Experiment

2.1. Aerosol collection

Mt. Hua is located in central China, and the sampling site is at the summit of the west peak (34°29' N, 110°05' E, 2060 m a.s.l., Fig. 1). The sampling campaign was performed on January 10–22, 2009 by using two air samplers (KC-120H, Qingdao Laoshan Company, China) for TSP and PM₁₀ collection at an airflow rate of 100 L min⁻¹ in each and one 8-stage size-segregated sampler (Thermoelectronic Company, USA) operating at 28.3 L min⁻¹ to collect the size-resolved aerosols with cutoff points as 0.4, 0.7, 1.1, 2.1, 3.3, 4.7, 5.8, and 9.0 μm. TSP and PM₁₀ were collected on a day/night basis each for 10 h, while the size-resolved aerosols were continuously collected for 4 days in each set. All the samples were collected using pre-combusted (450 °C for 6 h) quartz fiber filters. Field blanks were collected before and after the sampling by mounting the filters onto the three types of samplers for a few minutes without sucking any air. After sampling, the sample and the blank filters were transported into the laboratory and stored at -20 °C prior to analysis. Meteorological parameters, hourly monitored during the campaign, are shown in Table 1.

2.2. Measurements of elemental carbon (EC) and organic carbon (OC) in TSP and PM₁₀

OC and EC in the TSP and PM₁₀ samples were analyzed using DRI Model 2001 Carbon analyzer following the Interagency Monitoring of Protected Visual Environments (IMPROVE) thermal/optical reflectance (TOR) protocol (Chow et al., 2004, 2007). Briefly, a size of 0.526 cm² sample filter was put in a quartz boat inside the analyzer and stepwise heated to temperatures of 140 °C (OC1), 280 °C (OC2), 480 °C (OC3), and 580 °C (OC4) in a non-oxidizing helium (He) atmosphere, and 580 °C (EC1), 740 °C (EC2), and 840 °C (EC3) in an oxidizing atmosphere of 2% oxygen in helium. In addition, pyrolyzed carbon (PC) is determined by reflectance and transmittance of 633 nm light. The analyzer was calibrated with

Table 1

Meteorological data during the Mt. Hua sampling period^a.

	Daytime 0700–1800 local time			Nighttime 1900–0600 local time		
	Range	Mean	Std	Range	Mean	Std
Temperature, °C	-13.1–1.3	-2.8	3.8	-13.6–1.4	-4.4	4.2
Relative humidity, %	10–96	38	26	24–90	38	18
Pressure, hPa	790–803	797	4	787–803	797	4
Wind direction, deg	208–292	256	25	221–309	272	32
Wind speed, m s ⁻¹	1.6–8.9	4.9	2	3.7–10.6	6.9	2.2

^a Sampling period is 11–22 Jan. 2009. All the meteorological parameters were measured hourly. Std denotes standard deviation.

known quantities of CH₄ every day. One sample was randomly selected from every 10 samples and re-analyzed. Differences determined from the replicate analyses were <5% for TC, and <10% for OC and EC. Three blank filters were analyzed and subtracted from the ambient measurements. Primary organic carbon (POC) and secondary organic carbon (SOC) were calculated using the EC tracer method (Castro et al., 1999; Wang et al., 2010).

$$\text{POC} = \text{EC} * (\text{OC}/\text{EC})_{\min} \quad (1)$$

$$\text{SOC} = \text{OC} - \text{POC} \quad (2)$$

where (OC/EC)_{min} is the lowest value of OC/EC ratios.

2.3. Determination of inorganic ions in PM₁₀ and size-segregated samples

A size of 8.343 cm² punch aliquot from PM₁₀ sample and one quarter of size-segregated sample were extracted with 10 mL pure water respectively and filtered through a PTFE filter to remove the particles and filter debris. Then the water-extracts were determined for pH using a pH meter (HANNA HI8424 pH meter, US) at an ambient temperature of 25 °C and inorganic ions using an ion chromatography (Dionex 500, Dionex, US). Five cations (Na⁺, K⁺, NH₄⁺, Mg²⁺ and Ca²⁺) and six anions (F⁻, Cl⁻, Br⁻, NO₃⁻, NO₂⁻ and SO₄²⁻) were determined. The limits of detection were less than 0.05 mg L⁻¹ for anions and cations. Br⁻ and NO₂⁻ were not discussed in this paper because their mass concentrations were below the detection limit. Standard Reference Materials produced by the National Research Center for Certified Reference Materials, China were analyzed for quality assurance purpose. All data reported here

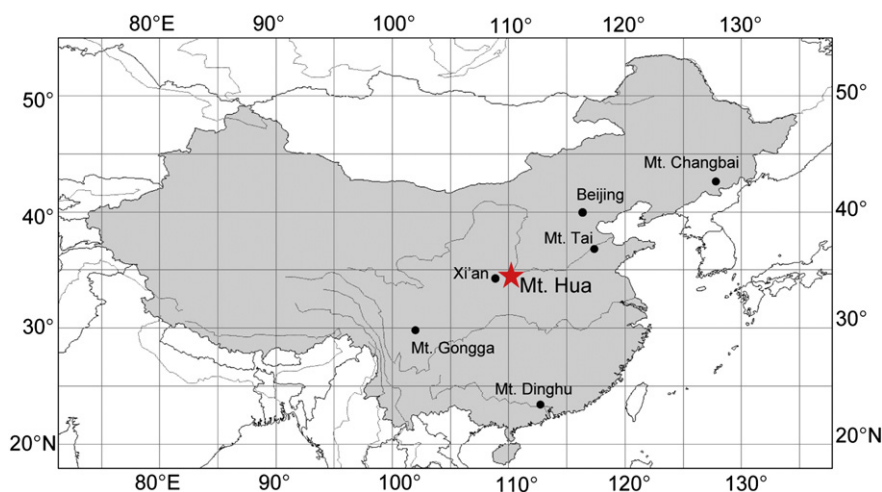


Fig. 1. Location of the sampling site at Mt. Hua in central China.

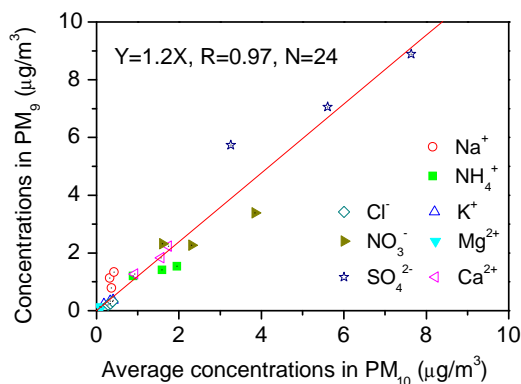


Fig. 2. An intercomparison of concentrations of the major compounds determined in the PM₁₀ samples and in the PM₉ fraction of the eight-stage samples (the sum of compound concentration in the stages of <0.4, 0.4–0.7, 0.7–1.1, 1.1–2.1, 2.1–3.3, 3.3–4.7, 4.7–5.8 and 5.8–9.0 µm). The denoted concentrations of species in PM₁₀ are the average of the samples collected during the period corresponding to the time which one set of the size-segregated samples were collected.

were subtracted by the field blanks. A strong linear correlation was obtained between the major ions in the PM₁₀ samples and in the summed size fractions (PM₉) of the size-segregated samples (Fig. 2), demonstrating a good consistency between the two data sets. However, concentrations of ions in the size-segregated samples are nearly 20% higher than those in PM₁₀, probably resulted from the loss of evaporation owing to the pressure drop in the PM₁₀ sampler (Wang et al., 2009b). Such a negative artifact has been reported (McMurry, 2000; Peters and Seifert, 1980).

3. Results and discussion

3.1. EC and OC in TSP and PM₁₀

Concentrations of OC and EC and OC/EC ratios in the TSP and PM₁₀ samples at the summit of Mt. Hua in winter are presented in

Table 2, along with the data from other alpine and lowland sites for a comparison. OC in TSP and PM₁₀ at the summit of Mt. Hua in winter were 6.9 ± 2.9 and 5.9 ± 2.5 $\mu\text{g m}^{-3}$, respectively. EC concentrations in TSP (0.9 ± 0.6 $\mu\text{g m}^{-3}$) and PM₁₀ (0.9 ± 0.5 $\mu\text{g m}^{-3}$) were almost equal, because EC is emitted from biomass and/or fossil fuel incomplete combustion processes as fine particles (Salma et al., 2004). OC and EC showed no significant day–night variation, but OC/EC ratios were higher in daytime (8.8 ± 3.8 in TSP and 7.1 ± 1.6 in PM₁₀, Table 2) than in nighttime (7.5 ± 1.5 in TSP and 6.1 ± 1.5 in PM₁₀), which was most likely due to an enhanced daytime secondary organic aerosol formation. OC and EC concentrations in Mt. Hua are 3–5 times higher than those in Mt. Cimone, Italy and Mt. Montseny, Spain, although OC/EC ratios at the three alpine sites are comparable (Table 2). The abundant carbonaceous aerosols in Mt. Hua are largely caused by the regional wintertime coal-burning emission due to house heating. In addition, OC and EC concentrations in Mt. Hua are almost 2 times higher than those in Zhuzhuang and Akdala (Table 2), two remote sites in China, most likely caused by an input of fossil fuel combustion emission from the nearby cities. As shown in Table 2, concentrations of OC and EC at the summit of Mt. Hua are around one order of magnitude lower than those from Chinese urban areas. OC/EC ratios at the summit of Mt. Hua (8.2 ± 3.0 in TSP and 6.6 ± 1.8 in PM₁₀) are similar to those (7.5–10.5) in the remote Chinese areas but 2–4 times higher than those in the urban regions. This is mainly due to far distance from EC sources (e.g., traffic and industrial emissions). On the other hand, the higher OC/EC ratio can also be explained by more organic particles formed by condensation due to lower temperature at the mountaintop and an enhanced photo-oxidation production of gaseous precursors during transport from lowlands onto the mountaintop, as well as an increased organic input from mountain plant emission.

OC in TSP and PM₁₀ well correlated each other (Fig. 3a, $R = 0.96$, $p < 0.001$), because the particles larger than 10 µm at the summit are negligible. However, such a good correlation was not observed for EC in TSP and PM₁₀ (Fig. 3b), which is mainly caused by the instrument measurement errors due to the low level of EC in the

Table 2

Concentrations of OC, EC and OC/EC ratios for TSP and PM₁₀ in the atmosphere over Mt. Hua and a comparison of EC and OC in PM₁₀ from different locations.

Locations	Sampling time		OC ($\mu\text{g m}^{-3}$)	EC ($\mu\text{g m}^{-3}$)	OC/EC
I Mountain sites and altitude					
Mt. Hua (TSP) ^a , China, 2160 m	Winter 2009	Day	6.6 ± 2.7	0.9 ± 0.5	8.8 ± 3.8
		Night	7.1 ± 3.1	1.0 ± 0.6	7.5 ± 1.5
		Average	6.9 ± 2.9	0.9 ± 0.6	8.2 ± 3.0
Mt. Hua (PM ₁₀) ^a , China, 2160 m		Day	6.0 ± 2.2	0.8 ± 0.4	7.1 ± 1.6
		Night	5.9 ± 2.7	0.9 ± 0.5	6.1 ± 1.5
		Average	5.9 ± 2.5	0.9 ± 0.5	6.6 ± 1.8
Mt. Cimone (PM ₁₀) ^b , Italy, 2165 m	Summer 2004		1.5	0.2	7.5
Montseny (PM ₁₀) ^c , Spain, 720m	Annual 2004–2007		2.1	0.2	10.5
II Remote sites					
Zhuzhang (PM ₁₀) ^d , China	Annual 2004–2005		3.1	0.34	9.1
Akdala (PM ₁₀) ^d , China	Annual 2004–2005		2.9	0.35	8.3
III Urban sites					
Xi'an (PM ₁₀) ^e , China	Winter 2003–2004		93.0	22.7	4.2
Beijing (PM ₁₀) ^f , China	Winter 2003		21.2	8.9	2.3
Guangzhou (PM ₁₀) ^g , China	Winter 2001		29.4	10.4	2.7
Zhuhai (PM ₁₀) ^g , China	Winter 2001		14.5	6.0	2.4
Shenzhen (PM ₁₀) ^g , China	Winter 2001		16.4	7.3	2.2
Hong Kong (PM ₁₀) ^g , China	Winter 2001		10.5	5.1	2.3

^a This study, $N = 21$.

^b Marenco et al., 2006.

^c Pey et al., 2009.

^d Qu et al., 2009.

^e Cao et al., 2005.

^f Zhang et al., 2007.

^g Cao et al., 2003.

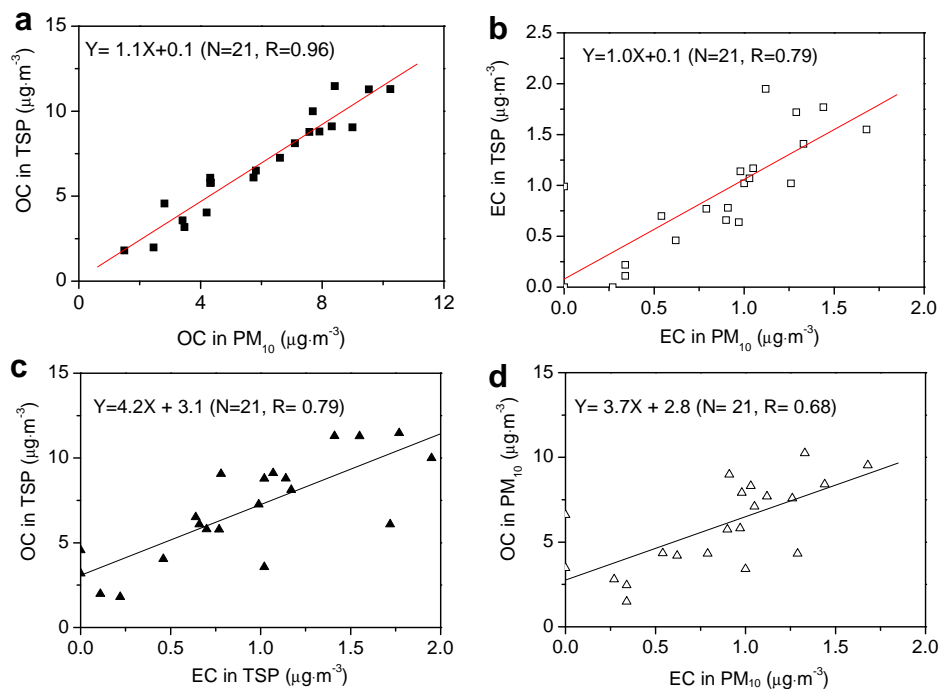


Fig. 3. The relationship between OC and EC in TSP and PM₁₀.

filter. Unlike those in urban areas (Cao et al., 2004; Li et al., 2008) OC and EC at the summit of Mt. Hua did not correlated well each other (Fig. 3c and d). OC and EC in urban areas are mostly resulted from common sources such as vehicle exhausts and coal burning emissions, and experience shorter time of atmospheric process such as deposition and degradation, thus their concentrations correlate well each other. In contrast, mountain aerosols in general experience longer time of atmospheric process during transport from lowland areas onto mountaintop with an additional input of organic aerosols emitted by mountain plants, resulting in the poor correlation between OC and EC.

POC in TSP and PM₁₀ in the atmosphere over Mt. Hua are 3.5 ± 1.7 and $3.2 \pm 1.3 \mu\text{g m}^{-3}$, while SOC are 3.7 ± 1.9 and $2.9 \pm 1.7 \mu\text{g m}^{-3}$, respectively (Fig. 4). SOC/POC ratios in the TSP and PM₁₀ samples are 1.3 ± 0.9 and 1.0 ± 0.5 , respectively, being 2–3 times higher than those (0.4–0.7) in the cities of China (Cao et al., 2007; Wang et al., 2010), again confirming an enhanced photochemical oxidation at the alpine site.

3.2. Inorganic ions of PM₁₀

Most inorganic ions except for NO₃⁻ showed slightly higher concentration in daytime than in nighttime (Table 3). Inorganic ions at the summit are mostly transported from lowland sources, thus more ions in daytime can be transported onto the mountaintop due to changes in the boundary layer heights. In addition, Na⁺ is higher than Cl⁻ in daytime but lower than Cl⁻ in nighttime. Besides sea salt source, sodium is also contained in soil dust (Mori et al., 2003; Sun et al., 2010), which can heterogeneously react with acidic gases (e.g., SO₂, NO_x) and form water-soluble Na⁺ especially in daytime when more soil dusts are transported onto the mountaintop. However, the lower concentration of nitrate in daytime may be ascribed to the increased volatilization compared to the case in nighttime under lower temperature. The averaged concentrations of total ions in PM₁₀ are $12.7 \pm 6.2 \mu\text{g m}^{-3}$ in winter with the orders of SO₄²⁻ > NO₃⁻ > NH₄⁺ > Ca²⁺ > Na⁺ > Cl⁻ > K⁺ > Mg²⁺ > F⁻ in daytime

and SO₄²⁻ > NO₃⁻ > NH₄⁺ > Ca²⁺ > Cl⁻ > K⁺ > Na⁺ > Mg²⁺ > F⁻ in nighttime. As shown in Table 3, ions concentrations at Mt. Hua are much lower than those in lowland urban sites, which can be ascribed to the loss by dry/wet deposition of aerosols and the dilution effect during transport from the lowlands to the mountaintop. Secondary ions (i.e., SO₄²⁻, NO₃⁻ and NH₄⁺) at the summit of Mt. Hua are 7–32 times higher than those in Waliguan (Table 3), a remote site in the country, but much lower than those in the summertime aerosols from the summit of Mt. Tai in east China (Xu et al., 2009). In general winter aerosols are more abundant than in summer, thus the higher loadings of ions at Mt. Tai in summer may indicate that aerosol pollution in east China is more serious than in the west, being consistent with those reported by satellite

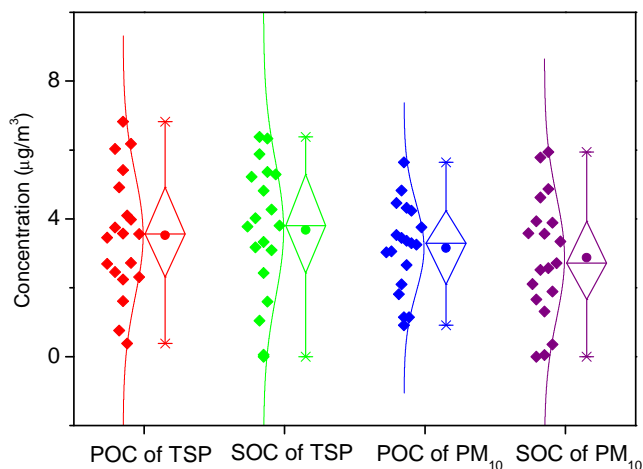


Fig. 4. Concentrations of primary (POC) and secondary organic carbon (SOC) in TSP and PM₁₀. The box plots indicate the mean 10-h concentration and the minimum, 1st, 25th, 50th, 75th, 99th and maximum percentiles. A normal curve was fitted to the measurements.

Table 3Concentrations of major ions ($\mu\text{g m}^{-3}$) in aerosols from Mt. Hua and other mountains in China and Europe, and a comparison with those in Chinese mega-cities.

Sampling site and altitude	Sampling time	SO_4^{2-}	NO_3^-	NH_4^+	Ca^{2+}	Cl^-	Na^+	K^+	Mg^{2+}	F^-	
I Mountain sites and altitude											
Mt. Hua (PM_{10}) ^a , Central China, 2160 m	Winter 2009	Day	6.0 ± 3.8	2.6 ± 1.7	1.6 ± 0.9	1.6 ± 0.7	0.4 ± 0.3	0.5 ± 0.3	0.3 ± 0.2	0.1 ± 0.0	0.1 ± 0.0
		Night	5.7 ± 3.5	2.9 ± 1.6	1.5 ± 0.9	1.4 ± 0.6	0.3 ± 0.2	0.2 ± 0.2	0.3 ± 0.2	0.1 ± 0.0	0.1 ± 0.0
		Mean	5.8 ± 3.6	2.7 ± 1.6	1.6 ± 0.9	1.5 ± 0.7	0.3 ± 0.2	0.4 ± 0.3	0.3 ± 0.2	0.1 ± 0.0	0.1 ± 0.0
Waliguan (TSP) ^b , Central China, 3816 m	Winter, 1995	0.19	0.01	0.24	na ⁱ	0.31	na	na	na	na	
Mt. Tai (TSP) ^c , East China, 1534 m	Summer 2006	20.05	13.72	9.72	6.67	3.13	1.08	3.21	0.33	na	
Mt. Gongga (PM_{10}) ^c , Southwest China, 3000 m	Summer 2006	4.42	0.79	1.47	0.07	0.23	0.13	0.21	0.45	na	
Mt. Dinghu (PM_{10}) ^c , South China, 1000 m	Summer 2006	7.88	1.74	2.65	0.35	0.45	0.56	0.37	0.08	na	
Mt. Changbai (PM_{10}) ^c , East China, 2691m	Summer 2006	2.79	0.52	1.11	0.09	0.34	0.04	0.12	0.02	na	
Mt. Cimone (PM_{10}) ^d , Italy, 2165 m	Summer 2004	3.5	0.8	1.4	na	na	na	na	na	na	
II Lowlands											
Hong Kong, China (PM_{10}) ^e	Winter 2000	15.3	4.9	3.3	na	na	na	na	na	na	
Xi'an, China(TSP) ^f	Winter 2006	40.8	21.9	13.6	9.1	7.7	2.0	4.1	1.0	1.1	
Nanjing, China ($\text{PM}_{2.5}$) ^g	Winter 2001	14.0	8.06	8.40	2.34	2.62	1.01	2.07	0.18	na	
Beijing, China ($\text{PM}_{2.5}$) ^h	Winter 2001–2003	20.96	12.29	10.64	1.68	5.28	0.88	2.48	0.20	0.55	

^a This study, $N = 21$.^b Yang et al., 1996.^c Xu et al., 2009.^d Marengo et al., 2006.^e Ho et al., 2003.^f Shen et al., 2008.^g Yang et al., 2005.^h Wang et al., 2005.ⁱ na: not available.

observations (Wittrock et al., 2006; Donkelaar et al., 2010). The ion concentrations at Mt. Hua in winter are comparable to those at Mt. Gongga, southwest China, Mt. Dinghu, south China and Mt. Changbai, northeast China, again indicating that air pollution in the east part of the country is most serious. SO_4^{2-} and NO_3^- at Mt. Hua are 1–3 times more abundant than those at Mt. Cimone in Italy (Table 3), which is most likely attributed to the heavy loadings of anthropogenic aerosols in China although the seasonal difference cannot be ruled out (Wang et al., 2006a).

A good linear correlation was observed between SO_4^{2-} and SOC ($R = 0.75$ during daytime and $R = 0.82$ during nighttime) (Fig. 5a), whereas a moderate linear correlation was found for NO_3^- and SOC ($R = 0.54$ and 0.62 in day and night, Fig. 5b). Many studies (Cao et al., 2005, 2007; Wang et al., 2010) have demonstrated that coal-burning emissions are still the major source of atmospheric aerosols in winter in China although vehicle numbers have sharply increased, which release a huge amount of SO_2 and organics. These pollutants can further be oxidized into sulfate and SOC via similar pathways such as in-cloud formation process (Yao et al., 2003), thus making both correlated well each other. Lower temperature and higher humidity are favorable to form particulate nitrate and sulfate, thus better correlations of both ions

with SOC were obtained at night compared with that in daytime (Fig. 5a and b).

3.3. Backward trajectories analysis

During the sampling period air mass at the mountain site were mostly transported northerly and northwesterly from Inner Mongolia and Sinkiang Autonomy of China (Fig. 6a), but air mass at the site on January 19, 2009 was transported from southern China (Fig. 6b). Thus all the samples could be classified into two groups: north and northwest group and south group. As seen in Table 4, all the components of PM_{10} except Ca^{2+} in the air mass transported from south China are 1–2 times more abundant than those from the north, suggesting aerosol pollution in south China is more serious. Humidity and temperature in southern China are higher than in the northern part, which is favorable for the formation of SO_4^{2-} from SO_2 , resulting in the aerosols from the south more acidic (Table 4 and Fig. 6b). In contrast, concentrations of Ca^{2+} showed a variation opposite to sulfate and nitrate, higher in the north and northwest air masses and lower in the south air mass (Table 4). That is because Ca^{2+} is mainly contained in dust aerosols (Shen et al., 2008, 2009), and aerosols transported from north and

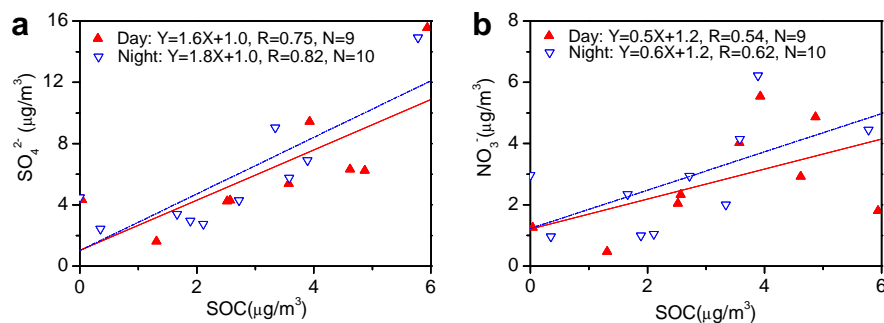


Fig. 5. Correlations of secondary organic carbon (SOC) with (a) sulfate and (b) nitrate during day and night (EC concentration in two samples was below the detection limit and not included for SOC calculation).

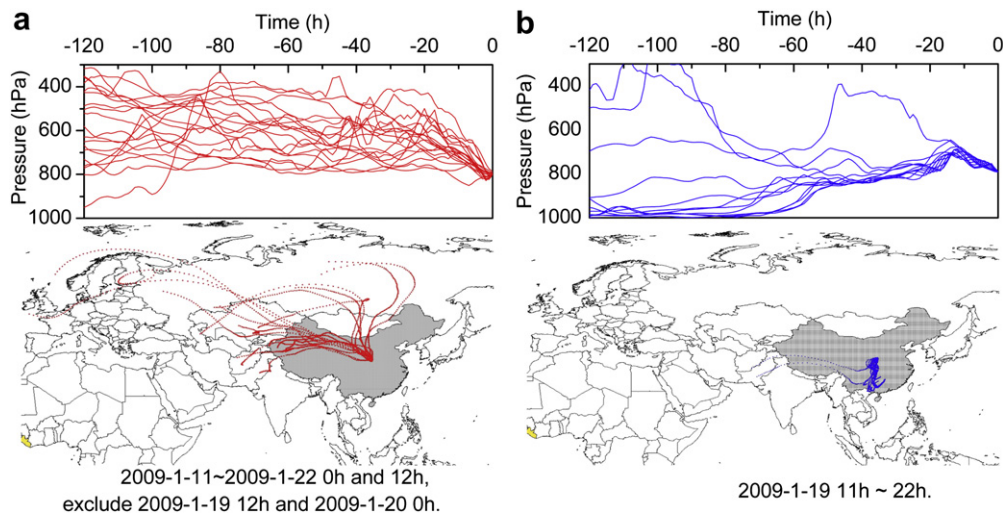


Fig. 6. 120-h backward air mass trajectories reaching Mt. Hua in winter ($34^{\circ}29' N$, $110^{\circ}05' E$, and the altitude was set as 2070 m): (a) 2009-1-11–2009-1-22 0 h and 12 h, exclude 2009-1-19 12 h and 2009-1-20 0 h; (b) 2009-1-19 11 h ~ 22 h.

northwester China are enriched with dust due to the proximity of desert source in the regions.

3.4. Size distributions of water-soluble inorganic ions

To further understand the chemical and physical characteristics of aerosols at the mountaintop, size-segregated samples were analyzed for water-soluble inorganic ions. Table 5 shows the concentrations and geometric mean diameters (GMD) of the ions in fine ($<2.1 \mu\text{m}$) and coarse ($\geq 2.1 \mu\text{m}$) particles. In the fine mode, SO_4^{2-} , NO_3^- , and NH_4^+ are the major components, accounting for 85% of the total ions. In contrast, ions in coarse mode are dominated by SO_4^{2-} , NO_3^- , and Ca^{2+} , indicating that ammonium mostly exists in fine particles. Ca^{2+} and Mg^{2+} (1.56 ± 0.29 and $0.09 \pm 0.01 \mu\text{g m}^{-3}$ in coarse mode) are major ions of soil dust and mostly presented in coarse particles. The coarse mode of Ca^{2+} and Mg^{2+} are largely produced by heterogeneous reactions of dust particles with acidic gases (e.g., HNO_3 and H_2SO_4) (Geng et al., 2009; Sun et al., 2010).

NH_4^+ and K^+ showed an unimodal size distribution in the fine mode, peaking at the range of $0.7\text{--}1.1 \mu\text{m}$ (Fig. 7a), while Ca^{2+} and Mg^{2+} displayed a coarse mode pattern, peaking at the range of $4.7\text{--}5.8 \mu\text{m}$ (Fig. 7b), being consistent with the results observed by Xu et al. (2009) at Mt. Tai in east China. Particulate ammonium is secondarily formed via heterogeneous reactions of gaseous ammonia with H_2SO_4 and HNO_3 , and mainly exists in accumulate mode of particles in form of $(\text{NH}_4)_2\text{SO}_4$, NH_4HSO_4 , and NH_4NO_3 , (Kerminen et al., 2001; Wang et al., 2006); thus GMD of sulfate, nitrate, and ammonium in fine mode are similar, which are 0.79,

0.81, and $0.81 \mu\text{m}$, respectively (Table 5). Potassium is mostly derived from biomass burning emission, which also occurs in fine particles.

Sulfate and nitrate mainly arise from photochemical oxidation of SO_2 and NO_x , and both present a large peak at the range of $0.7\text{--}1.1 \mu\text{m}$ (Fig. 7c), and a small peak at the size of $4.7\text{--}5.8 \mu\text{m}$. Sulfate is initially formed as a condensation mode by in-cloud process and subsequently grows into $0.7\text{--}1.1 \mu\text{m}$ as a droplet mode by uptake of water (John et al., 1990). Size distribution of nitrate is mainly influenced by the thermodynamic equilibrium of $\text{HNO}_3(\text{g}) + \text{NH}_3(\text{g}) \rightleftharpoons \text{NH}_4\text{NO}_3(\text{s, aq})$. The low temperature at the summit of Mt. Hua in winter is favorable for the formation of particulate $\text{NH}_4\text{NO}_3(\text{s, aq})$, so the size range of primary peak of nitrate is coincident with that of ammonium (Fig. 7a and c). However, the secondary peak of NO_3^- may be caused by the adsorption of gaseous HNO_3 onto coarse particles that contain alkaline species like Na, Ca, Mg and K (Fig. 7c). Na^+ and Cl^- showed a bimodal distribution with two equivalent peaks at the ranges of $0.7\text{--}1.1$ and $4.7\text{--}5.8 \mu\text{m}$. The coarse mode of Na^+ and Cl^- is possibly originated from particles emitted from dried saline lakes in north and northwest China, because Mt. Hua is located in inland China and influence of air masses from ocean is insignificant especially in winter. However, their fine mode origins are unclear.

Size distribution of cation/anion equivalent ratio and ΔpH were also shown in Fig. 7e and f. In the fine mode ($<2.1 \mu\text{m}$) the cation/anion equivalent ratio was slightly lower than unity (Fig. 7e)

Table 4

Concentrations of major species ($\mu\text{g m}^{-3}$) and ΔpH in PM_{10} from northerly and southerly air masses and their ratios in different air masses.

	Northerly ($N = 19$)	Southerly ($N = 2$)	S/N ratio ^a
OC	5.6 ± 2.3	9.6 ± 0.6	1.7
EC	0.8 ± 0.5	1.1 ± 0.2	1.4
SO_4^{2-}	4.8 ± 2.1	15.2 ± 0.3	3.2
NO_3^-	2.7 ± 1.6	3.1 ± 1.3	1.2
NH_4^+	1.4 ± 0.7	3.3 ± 0.0	2.4
Ca^{2+}	1.5 ± 0.7	1.4 ± 0.0	0.9
ΔpH	0.0 ± 0.2	-1.3 ± 0.2	

^a Ratios of concentrations in air mass transported from southerly to that from northerly.

Table 5

Concentrations and geometric mean diameters (GMD)^a of ions in fine ($<2.1 \mu\text{m}$) and coarse ($\geq 2.1 \mu\text{m}$) modes of particles at the summit of Mt. Hua.

$N = 3$	Concentration ($\mu\text{g m}^{-3}$)		GMD (μm)	
	Fine	Coarse	Fine	Coarse
Na^+	0.54 ± 0.25	0.58 ± 0.09	0.71 ± 0.04	6.23 ± 1.57
NH_4^+	1.29 ± 0.13	0.11 ± 0.01	0.81 ± 0.12	6.89 ± 0.23
K^+	0.28 ± 0.05	0.03 ± 0.01	0.85 ± 0.06	7.67 ± 1.55
Mg^{2+}	0.05 ± 0.01	0.09 ± 0.01	1.01 ± 0.13	7.06 ± 0.92
Ca^{2+}	0.42 ± 0.05	1.56 ± 0.29	0.86 ± 0.03	8.26 ± 0.40
Cl^-	0.15 ± 0.02	0.13 ± 0.07	0.71 ± 0.13	11.91 ± 4.38
NO_3^-	1.60 ± 0.53	1.22 ± 0.14	0.81 ± 0.06	7.49 ± 0.23
SO_4^{2-}	4.99 ± 0.55	2.44 ± 0.70	0.79 ± 0.10	6.72 ± 0.46

^a $\log\text{GMD} = (\sum C_i \log D_{p_i}) / \sum C_i$, where C_i is the concentration of compound in size i and D_{p_i} is the geometric mean particle diameter collected on stage i (Hinds, 1999).

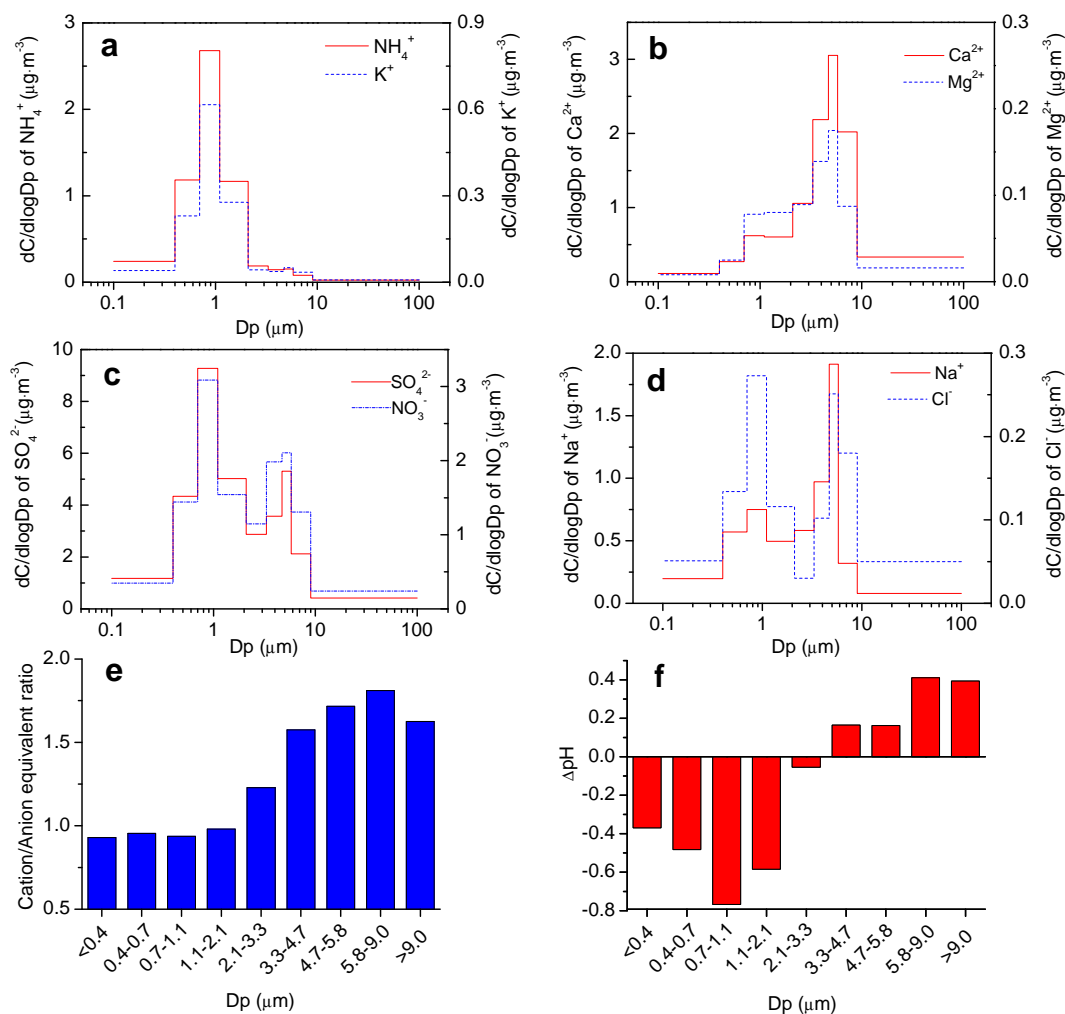


Fig. 7. Size distributions of (a–d) water-soluble ions, (e) cation/anion equivalent ratio, and (f) ΔpH of water-extracts in PM_{10} .

and ΔpH presented negative values (Fig. 7f), being opposite to those in the coarse mode. The pH values showed that the mountain aerosols in diameter of $0.7\text{--}1.1\ \mu\text{m}$ are most acidic, in which anions have the highest concentration compared to cations.

4. Conclusion

Concentrations of OC in TSP and PM_{10} at the summit of Mt. Hua in winter were 6.9 ± 2.9 and $5.9 \pm 2.5\ \mu\text{g}\ \text{m}^{-3}$, while EC were 0.9 ± 0.6 and $0.9 \pm 0.5\ \mu\text{g}\ \text{m}^{-3}$, respectively. SO_4^{2-} , NO_3^- , NH_4^+ and Ca^{2+} were found to be the major ions in PM_{10} with concentrations of 5.8 ± 3.7 , 2.7 ± 1.6 , 1.6 ± 0.9 and $1.5 \pm 0.7\ \mu\text{g}\ \text{m}^{-3}$, respectively. High SOC/POC ratios (1.3 ± 0.9 in TSP and 1.0 ± 0.5 in PM_{10}) were observed at the summit, indicating an increased photo-oxidation production during the transport process of organic precursors from lowland surface to the mountaintop. Compared with that from north China air masses transported from south China contained higher concentrations of SO_4^{2-} and NH_4^+ and lower concentration of Ca^{2+} . Size distributions of NH_4^+ and K^+ presented an accumulation mode with a peak at $0.7\text{--}1.1\ \mu\text{m}$, in contrast to Ca^{2+} and Mg^{2+} , which displayed a coarse mode pattern with a peak in the size of $4.7\text{--}5.8\ \mu\text{m}$. SO_4^{2-} , NO_3^- , Na^+ and Cl^- at the mountaintop showed a bimodal pattern, peaking at $0.7\text{--}1.1\ \mu\text{m}$ in fine mode and $4.7\text{--}5.8\ \mu\text{m}$ in coarse mode. pH values of the water-extracts suggest

that aerosols derived from north/northwest China are less acidic than those from the south, and particles with diameter of $0.7\text{--}1.1\ \mu\text{m}$ are most acidic, in which anions have the highest concentration compared to cations.

Acknowledgements

This work was financially supported by China Natural Science Foundation (No. 40873083), the Knowledge Innovation Program of Chinese Academy of Sciences (No. kzcx2-yw-148).

References

- Aldhous, P., 2005. China's burning ambition. *Nature* 435, 1152–1154.
- Arimoto, R., Kim, Y.J., Kim, Y.P., Quinn, P.K., Bates, T.S., Anderson, T.L., Gong, S., Uno, I., Chin, M., Huebert, B.J., Clarke, A.D., Shinzuka, Y., Weber, R.J., Anderson, J.R., Guazzotti, S.A., Sullivan, R.C., Sodeman, D.A., Prather, K.A., Sokolik, I.N., 2006. Characterization of Asian dust during ACE-Asia. *Global and Planetary Change* 52 (1–4), 23–56.
- Cao, J.J., Lee, S.C., Ho, K.F., Zhang, X.Y., Zou, S.C., Fung, K.K., Chow, J.C., Watson, J.G., 2003. Characteristics of carbonaceous aerosol in Pearl River Delta region, China during 2001 winter period. *Atmospheric Environment* 37, 1451–1460.
- Cao, J.J., Lee, S.C., Ho, K.F., Zou, S.C., Fung, K.K., Li, Y., Watson, J.G., Chow, J.C., 2004. Spatial and seasonal variations of atmospheric organic carbon and elemental carbon in Pearl River Delta region, China. *Atmospheric Environment* 38, 4447–4456.

- Cao, J.J., Wu, F., Chow, J.C., Lee, S.C., Li, Y., Chen, S.W., An, Z.S., Fung, K.K., Watson, J.G., Zhu, C.S., Liu, S.X., 2005. Characterization and source apportionment of atmospheric organic and elemental carbon during fall and winter of 2003 in Xi'an, China. *Atmospheric Chemistry and Physics* 5, 3127–3137.
- Cao, J.J., Lee, S.C., Chow, J.C., Watson, J.G., Ho, K.F., Zhang, R.J., Jin, Z.D., Shen, Z.X., Chen, G.C., Kang, Y.M., Zou, S.C., Zhang, L.Z., Qi, S.H., Dai, M.H., Cheng, Y., Hu, K., 2007. Spatial and seasonal distributions of carbonaceous aerosols over China. *Journal of Geophysical Research* 112, D22S11. doi:10.1029/2006JD008205.
- Castro, L.M., Pio, C.A., Harrison, R.M., Smith, D.J.T., 1999. Carbonaceous aerosol in urban and rural European atmospheres: estimation of secondary organic carbon concentrations. *Atmospheric Environment* 33, 2771–2781.
- Chow, J.C., Watson, J.G., Chen, L.-W.A., Arnott, W.P., Moosmuller, H., Fung, K.K., 2004. Equivalence of elemental carbon by thermal/optical reflectance and transmittance with different temperature protocols. *Environmental Science and Technology* 38, 4414–4422.
- Chow, J.C., Watson, J.G., Chen, L.-W.A., Chang, M.C.O., Robinson, N.F., Trimble, D., Kohl, S., 2007. The IMPROVE-A temperature protocol for thermal/optical carbon analysis: maintaining consistency with a long-term database. *Journal of the Air and Waste Management Association* 57, 1014–1023.
- Donkelaar, A.V., Martin, R.V., Brauer, M., Kahn, R., Levy, R., Verduzco, C., 2010. Global estimates of ambient fine particulate matter concentrations from satellite-based aerosol optical depth: development and application. *Environmental Health Perspectives* 118, 847–855.
- Duan, F.K., He, K.B., Ma, Y.L., Jia, Y.T., Yang, F.M., Lei, Y., Tanaka, S., Okuta, T., 2005. Characteristics of carbonaceous aerosols in Beijing, China. *Chemosphere* 60, 355–364.
- Geng, H., Park, Y., Hwang, H., Kang, S., Ro, C.U., 2009. Elevated nitrogen-containing particles observed in Asian dust aerosol samples collected at the marine boundary layer of the Bohai sea and the Yellow sea. *Atmospheric Chemistry and Physics* 9, 6933–6947.
- Hinds, W.C., 1999. *Aerosol Technology: Properties, Behavior, and Measurement of Airborne Particles*. John Wiley and Sons, New York.
- Ho, K.F., Lee, S.C., Chan, C.K., Yu, J.C., Chow, J.C., Yao, X.H., 2003. Characterization of chemical species in PM_{2.5} and PM₁₀ aerosols in Hong Kong. *Atmospheric Environment* 37, 31–39.
- John, W., Wall, S.M., Ondo, J.L., Winklmayr, W., 1990. Modes in the size distributions of atmospheric inorganic aerosol. *Atmospheric Environment* 24A, 2349–2359.
- Kerminen, V., Hillamo, R., Teinilä, K., Pakkanen, T., Allegrini, I., Sparapani, R., 2001. Ion balances of size-resolved tropospheric aerosol samples: implications for the acidity and atmospheric processing of aerosols. *Atmospheric Environment* 35, 5255–5265.
- Li, J., Zhuang, G.S., Huang, K., Lin, Y.F., Xu, C., Yu, S.L., 2008. Characteristics and sources of air-borne particulate in Urumqi, China, the upstream area of Asia dust. *Atmospheric Environment* 42, 776–787.
- Marenco, P., Bonasoni, F., Calzolari, M., Ceriani, M., Chiari, J., Cristofanelli, P., 2006. Characterization of atmospheric aerosols at Monte Cimone, Italy, during summer 2004: source apportionment and transport mechanisms. *Journal of Geophysical Research* 111, D24202. doi:10.1029/2006JD007145.
- Menon, S., Hansen, J., Nazarenko, L., Luo, Y., 2002. Climate effects of black carbon aerosols in China and India. *Science* 297, 2250–2253.
- McMurry, P.H., 2000. A review of atmospheric aerosol measurements. *Atmospheric Environment* 34, 1959–1999.
- Mori, I., Nishikawa, M., Tanimura, T., Quan, H., 2003. Change in size distribution and chemical composition of kosa (Asian dust) aerosol during long-range transport. *Atmospheric Environment* 37, 4253–4263.
- Peters, J., Seifert, J.H., 1980. Losses of benzo(a)pyrene under the conditions of high-volume sampling. *Atmospheric Environment* 14, 117–120.
- Pey, J., Pérez, N., Castillo, S., Viana, M., Moreno, T., Pandolfi, M., López-Sebastián, J.M., Alastuey, A., Querol, X., 2009. Geochemistry of regional background aerosols in the western Mediterranean. *Atmospheric Research* 94, 422–435.
- Qu, W.J., Zhang, X.Y., Arimoto, R., Wang, Y.Q., Wang, D., Sheng, L.F., Fu, G., 2009. Aerosol background at two remote CAWNET sites in western China. *Science of the Total Environment* 407, 3518–3529.
- Rosenfeld, D., Dai, J., Yu, X., Yao, Z., Xu, X., Yang, X., Du, C., 2007. Inverse Relations between amounts of air pollution and Orographic precipitation. *Science* 315, 1396–1398.
- Salma, I., Chi, X.G., Maenhaut, W., 2004. Elemental and organic carbon in urban canyon and background environments in Budapest, Hungary. *Atmospheric Environment* 38, 27–36.
- Shen, Z.X., Arimoto, R., Cao, J.J., Zhang, R.J., Li, X.X., Du, N., Okuda, T., Nakao, S., Tanaka, S., 2008. Seasonal variations and evidence for the effectiveness of pollution controls on water-soluble inorganic species in total suspended particulates and fine particulate matter from Xi'an, China. *Journal of the Air & Waste Management Association* 58, 1560–1570.
- Shen, Z.X., Cao, J.J., Arimoto, R., Han, Z.W., Zhang, R.J., Han, Y.M., Liu, S.X., Okuda, T., Nakao, S., Tanaka, S., 2009. Ionic composition of TSP and PM_{2.5} during dust storms and air pollution episodes at Xi'an, China. *Atmospheric Environment* 43, 2911–2918.
- Sun, Y.L., Zhuang, G.S., Wang, Y., Zhao, X.J., Li, J., Wang, Z.F., An, Z.S., 2005. Chemical composition of dust storms in Beijing and implications for the mixing of mineral aerosol with pollution aerosol on the pathway. *Journal of Geophysical Research* 110, D24209. doi:10.1029/2005JD006054.
- Sun, Y.L., Zhuang, G.S., Huang, K., Li, J.A., Wang, Q.Z., Wang, Y., Lin, Y.F., Fu, J.S., Zhang, W.J., Tang, A.H., Zhao, X.J., 2010. Asian dust over northern China and its impact on the downstream aerosol chemistry in 2004. *Journal of Geophysical Research-Atmospheres* 115, D00K09. doi:10.1029/2009JD012757.
- Wang, G.H., Kawamura, K., Watanabe, T., Lee, S.C., Ho, K.F., Cao, J.J., 2006a. Heavy loadings and source strengths of organic aerosols in China. *Geophysical Research Letters* 33, L22801. doi:10.1029/2006GL027624.
- Wang, G.H., Kawamura, K., Lee, S.C., Ho, K.F., Cao, J.J., 2006b. Molecular, seasonal and spatial distributions of organic aerosols from fourteen Chinese cities. *Environmental Science & Technology* 40, 4619–4625.
- Wang, G.H., Kawamura, K., Xie, M., Hu, S., Gao, S., Cao, J., An, Z., Wang, Z., 2009a. Size-distributions of n-alkanes, PAHs and hopanes and their sources in the urban, mountain and marine atmospheres over East Asia. *Atmospheric Chemistry and Physics* 9, 8869–8882.
- Wang, G.H., Kawamura, K., Umemoto, N., Xie, M., Hu, S., Wang, Z., 2009b. Water-soluble organic compounds in PM_{2.5} and size-segregated aerosols over Mount Tai in north China Plain. *Journal of Geophysical Research* 114, D19208. doi:10.1029/2008JD011390.
- Wang, G.H., Xie, M., Hu, S., Tachibana, E., Kawamura, K., 2010. Dicarboxylic acids, metals and isotopic compositions of C and N in atmospheric aerosols from inland China: implications for dust and coal burning emission and secondary aerosol formation. *Atmospheric Chemistry and Physics Discuss* 10, 6895–6921.
- Wang, Y., Zhuang, G.S., Tang, A.H., Yuan, H., Sun, Y.L., Chen, S.A., Zheng, A.H., 2005. The ion chemistry and the source of PM_{2.5} aerosol in Beijing. *Atmospheric Environment* 39, 3771–3784.
- Wang, Y., Zhuang, G.S., Zhang, X.Y., Huang, K., Xu, C., Tang, A.H., Chen, J.M., An, Z.S., 2006. The ion chemistry, seasonal cycle, and sources of PM_{2.5} and TSP aerosol in Shanghai. *Atmospheric Environment* 40, 2935–2952.
- Wittrock, F., Richter, A., Oetjen, H., Burrows, J.P., Kanakidou, M., Myriokefalitakis, S., Volkamer, R., Beirle, S., Platt, U., Wagner, T., 2006. Simultaneous global observations of glyoxal and formaldehyde from space. *Geophysical Research Letters* 33, L16804. doi:10.1029/2006GL026310.
- Xu, H., Wang, Y., Wen, T., Yang, Y., Zhao, Y., 2009. Characteristics and source apportionment of atmospheric aerosols at the summit of Mount Tai during summertime. *Atmospheric Chemistry and Physics Discuss* 9, 16361–16379.
- Yang, D.Z., Yu, X.L., Fang, X.M., Wu, F., Li, X.S., 1996. A study of aerosol at regional background stations and baseline station. *Quarterly Journal of Applied Meteorology* 7 (4), 396–405 (in Chinese).
- Yang, H., Yu, J.Z., Ho, S.S.H., Xu, J.H., Wu, W.S., Wan, C.H., Wang, X.D., Wang, X.R., Wang, L.S., 2005. The chemical composition of inorganic and carbonaceous materials in PM_{2.5} in Nanjing, China. *Atmospheric Environment* 39, 3735–3749.
- Yao, X.H., Chan, C.K., Fang, M., Cadle, S., Chan, T., Mulawa, P., He, K.B., Ye, B.M., 2002. The water-soluble ionic composition of PM_{2.5} in Shanghai and Beijing, China. *Atmospheric Environment* 36, 4223–4234.
- Yao, X.H., Lau, Arthur P.S., Fang, M., Chan, C.K., Hu, M., 2003. Size distributions and formation of ionic species in atmospheric particulate pollutants in Beijing, China: 1—inorganic ions. *Atmospheric Environment* 37, 2991–3000.
- Zhang, R.J., Cao, J.J., Lee, S.C., Shen, Z.X., Ho, K.F., 2007. Carbonaceous aerosols in PM₁₀ and pollution gases in winter in Beijing. *Journal of Environmental Science* 19 (5), 564–571.